THE JOURNAL OF PHYSICAL CHEMISTRY B

Article

pubs.acs.org/JPCB

Synchrotron Small-Angle X-ray Scattering Studies of Hemoglobin Nonaggregation Confined inside Polymer Capsules

Soumit S. Mandal,[†] Satarupa Bhaduri,*[,†] Heinz Amenitsch,[‡] and Aninda J. Bhattacharyya[†,§]

[†]Solid State and Structural Chemistry Unit, Indian Institute of Science, Bangalore 560012, India

[‡]Institute of Biophysics and Nanosystems Research, Austrian Academy of Sciences, Schmiedlstrasse 6, A-8042, Graz, Austria

Supporting Information

ABSTRACT: The effect of confinement on the structure of hemoglobin (Hb) within polymer capsules was investigated here. Hemoglobin transformed from an aggregated state in solution to a nonaggregated state when confined inside the polymer capsules. This was directly confirmed using synchrotron small-angle X-ray scattering (SAXS) studies. The radius of gyration (R_g) and polydispersity (p) of the proteins in the confined state were smaller compared to those in solution. In fact, the R_g value is very similar to theoretical values obtained using protein structures generated from the Protein Databank. In the temperature range (25−85 °C, Tm 59 °C), the R_g values for the confined Hb remained constant. This observation is in contrary to the increasing R_g values obtained for the bare Hb in solution. This suggested higher thermal stability of Hb when confined inside the polymer capsule than when in solution. Changes in protein configuration were also reflected in the protein function. Confinement resulted in a beneficial enhancement of the electroactivity of Hb. While Hb in solution showed dominance of the cathodic process ($Fe^{3+} \rightarrow Fe^{2+}$), efficient reversible Fe^{3+}/Fe^{2+} redox response is observed in the case of the confined Hb. This has important protein functional implications. Confinement allows the electroactive heme to take up positions favorable for various biochemical activities such as sensing of analytes of various sizes from small to macromolecules and controlled delivery of drugs.

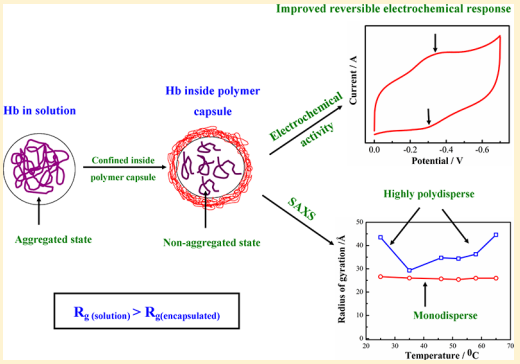

INTRODUCTION

Study of macromolecules such as proteins under confinement is a subject of considerable interest due to its direct association with various fields of biotechnology.[1] Confining proteins or in general biomacromolecules inside artificially created hosts is an effective approach for mimicking living cells.[2] This facilitates controlled study of various biological phenomena attached with the protein function. Proteins can be suitably confined in a variety of inorganic, organic, and even inorganic−organic hybrid matrixes. An overwhelming number of studies have concentrated on the protein function under confinement. The protein function has been primarily attributed to the interplay of a large number of parameters related to both the protein and the host. Key factors controlling the function of confined proteins are intermolecular (protein−protein) interaction,[3] protein−host interaction,[4] and confined solvent[5] configurations. Theoretically, these issues have been largely accounted for in the context of excluded volume, macromolecular crowding, and solvation.[6] It is believed that factors affecting protein function are a consequence of changes in protein structure. Under confinement, the population of the molecules is reduced (from Avogadro number, N0). Further reduced space would also result in lower conformational entropy restricting the molecule to fewer allowed conformations compared to the bulk. Eggers et al.[7] studied the effects of pH and ionic strength on the secondary structure of apomyoglobin confined in silica matrix. Protein conformations were observed to be influenced directly by the properties of confined water inside the pores of the matrix.[8] We demonstrate here the changes in hemoglobin aggregation (tertiary structure) as a result of its confinement inside polymer capsules. Synchrotron small-angle X-ray scattering (SAXS) analysis was done to account for the structural changes between Hb in solution and that confined inside polymer capsules. The changes in structure were manifested via changes in protein function as evidenced from electrochemical and spectroscopic investigations.

EXPERIMENTAL: METHODS AND MATERIALS

Preparation of Polymer Capsules. The polymer capsules were synthesized using a layer-by-layer approach on silica template. The silica templates (spheres) were synthesized using a standard method described in ref 9. The silica spheres were dispersed in water by sonication prior to coating with polymeric layers. The washed silica particles were then dispersed alternately in chitosan solution (1 mg/mL) adjusted to pH 5 and alginic acid solution (1 mg/mL) adjusted to pH 5 (pK_a of chitosan 6.5 and alginic acid 3.5). This process was repeated until 10 bilayers were deposited. All coating steps were

Received: April 14, 2012
Revised: July 22, 2012
Published: July 23, 2012

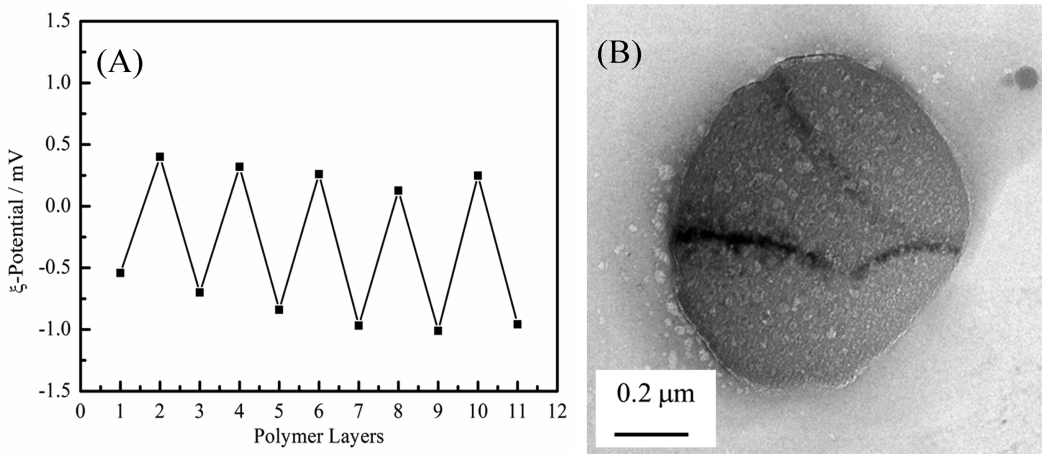

Figure 1. (A) Variation in ζ-potential with progressive coating of the silica templates with chitosan and alginic acid polymers monitored up to 10 layers. (B) Transmission electron microscope (TEM) image showing the general morphology of the polymer capsules (in dry state) after leaching out the silica template. Dark patches on the polymer capsule surface arise mostly due to folding after drying.

performed with constant vortexing by washing with water. For removal of the silica core, the polymer coated silica particles were suspended in 4 M NaOH solution and kept at slow vortexing overnight. The polymer capsules were obtained by removing the NaOH by centrifugation followed by washing with water.

Encapsulation of Hemoglobin in Polymeric Capsules. The polymer capsules were incubated with 5 mg/mL solution of hemoglobin (Human Hb, M.W. 65000) in PBS buffer (0.1 M, pH 7.0) and kept at 40 °C overnight. Following this, the solution was centrifuged to remove the supernatant and the polymer capsules were redispersed in PBS buffer. Hereafter, polymer capsules impregnated with Hb have been abbreviated as Hb-poly.

Preparation of Modified Working Electrode for Cyclic Voltammetry. Prior to modification, glassy carbon electrode (GCE, diameter: 3 mm) was polished with 0.3 μm alumina slurry to a mirror finish. After each polishing step, the electrode was rinsed and ultrasonicated, respectively, in ethanol and redistilled water for 60 s. A 20 μL portion of Hb-poly and Hb was dropped on the shining surface of GCE and dried for 3−4 h in air at room temperature followed by drying for 2 h in a desiccator. The cyclic voltammetry measurements were carried out using an electrochemical workstation CHI608 (CH Instruments). Hb-poly/GCE and Hb/GCE were used as the working electrode. The counter and reference electrodes were Pt wire and saturated calomel electrode (SCE), respectively. The working solution (5 mL of 0.1 M PBS, pH 7.0) was deoxygenated prior to the start of the measurement. The N_2 atmosphere was maintained during the course of measurement.

Characterization of the Polymer Capsules and the Confined Protein. *Electron Microscopy.* The scanning electron microscopy (SEM) analysis for the silica spheres was carried out using ESEM Quanta in the voltage range 5−10 kV. Transmission electron microscope (TEM) images were observed and recorded on a FEI Tecnai T-20 with an acceleration voltage of 200 kV. A 2 μL portion of sample solution was dropped on a Cu grid with a carbon-reinforced plastic film.

Zeta Potential (ζ) Measurement. The zeta potential of the polymer capsules was determined at each adsorption step in the layer-by-layer coating procedure with a Malvern Zetasizer (ZEN 3690). All measurements were performed at room temperature using Millipore water (specific resistance around 18 MΩ cm). The zeta potential value was taken from the average of three consecutive measurements.

Ultraviolet (UV−vis) Spectroscopy. The UV−vis spectroscopy was carried out using a Nanodrop spectrophotometer (ND-1000). The amount of confined Hb within the polymer capsule was estimated from the difference in absorption at 280 nm of the parent Hb solution used for incubation and the supernatant obtained after incubation. The molar extinction coefficient (ε) value (=25 565 M^{-1} cm^{-1}) was used to finally convert the absorbance values to the concentration.

Confocal Laser Scanning Microscopy (CLSM). CLSM imaging was carried out using a Zeiss 510 Meta confocal microscope (60× objective) to establish the structure of the polymer capsules as well as loading of the protein in it. The hemoglobin was tagged with a fluorescent dye fluorescein isothiocyanate (FITC) using a procedure described in ref 10. This tagged protein was incubated with the polymer capsules at pH 5 and 8. These polymer samples were then dropped onto a microscopic glass slide and covered with a coverslip. The edge of the coverslip was sealed with nail paint, and then, the slide was analyzed under CLSM using an excitation wavelength of 488 nm.

Circular Dichroism. 20 μL of Hb and Hb-poly samples were mixed with 380 μL of the fresh buffer. 200 μL of this solution was taken in a 1 mm cuvette for recording the CD spectrum (JASCO J-715). A temperature dependent CD spectrum was also recorded by monitoring the signal at 222 nm as a function of temperature between 25 and 85 °C at 1 °C/min interval.

Small-Angle X-ray Scattering (SAXS). The synchrotron SAXS (Austrian SAXS beamline[11] at the Italian synchrotron center, ELETTRA, Trieste, operated at 2 GeV) was carried out using a Pilatus detector. The sample-to-detector distance was kept at 1 m, and an X-ray energy of 8 keV was used. SAXS was recorded in the q range 0.01−0.15 $Å^{-1}$. Silver behenate ($CH_3(CH_2)_{20}COOAg$) with a d-spacing of 58.38 Å was used as a standard to calibrate the angular scale of the 2-D detector. PBS buffer solutions were selected in all cases as the background. The solutions have been measured in the same glass capillary (⌀ 1.5 mm). During data analysis, CRYSOL[12] was used to simulate scattering profiles from atomic coordinates. The scattering profiles were also recorded as a function of temperature in the range 25−75 °C using a

dx.doi.org/10.1021/jp303596q | J. Phys. Chem. B 2012, 116, 9604−9610

temperature bath (Unistat, Huber, Germany) connected to the sample holder.

RESULTS AND DISCUSSION

Characterization of the Polymer Capsules Templated on Silica Cores and Encapsulation of the Protein in Polymer Capsules. From SEM, silica cores were observed to be approximately 10 μm in diameter (Supporting Information; Figure S2). The stepwise coating of silica cores with chitosan and alginic acid was monitored by measuring the ζ-potential at each coating step (Figure 1A). In the beginning, the uncoated silica spheres exhibited a ζ-potential of −0.55 mV which changed to a positive potential 0.42 mV upon deposition of a layer of chitosan. This value again changed to a negative potential of −0.7 mV following the deposition of alginic acid layer. With progressive coating, the ζ-potential kept switching between −1.0 and 0.5 mV, indicating the deposition of the positively charged chitosan and the negatively charged alginic acid. After 10 bilayers of deposition (i.e., 10 layers each of chitosan and alginic acid), the silica core was removed using 4 M NaOH solution. Figure 1B shows the TEM image of the dry polymer capsules following the removal of silica cores. The distorted appearance of polymer capsules is attributed to the dry state which is a necessary prerequisite for the TEM measurement.

The encapsulation of the protein within the polymer capsules was established by CLSM microscopy. At pH 5 (Figure 2A),

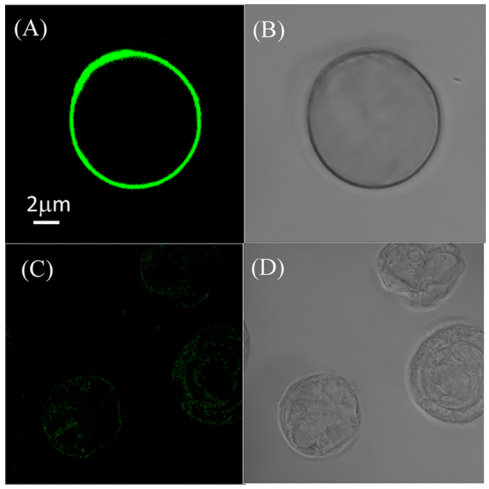

Figure 2. Confocal laser scanning microscopy (CLSM) images showing the polymer capsules with FITC labeled Hb at (A, dark field; B, bright field) pH 5 and (C, dark field; D, bright field) pH 8.

the fluorescein isothiocyanate (FITC, excitation wavelength of 488 nm) tagged protein is observed to be adsorbed on the outer surface of the polymer capsule, inferring hollowness of the spherically shaped polymer capsule. At pH 8, the protein was observed to penetrate inside the polymer capsule as a result of which the fluorescence arises from the protein present inside the polymer capsule (Figure 2C). pH 7 (not discussed here) resulted in an intermediate situation with the protein being partly attached outside the capsule and partly inside. This can be explained by taking into account the pK_a values of the chitosan and alginic acid. The chitosan has a pK_a of 6.5, while that for alginic acid is 1.5−3.5. Thus, at pH 5, the chitosan is positively charged, while the alginic acid is negatively charged. Thus, there is a very strong electrostatic attractive force between the oppositely charged polymer layers. This leads to a very compact polymer capsule, and the tagged Hb is unable to penetrate inside the capsule. While at pH 8, the chitosan layer is neutral but the alginic acid layer is negatively charged. Thus, the repulsion between the adjacent alginic acid layers creates pores in the polymer capsule allowing the Hb to diffuse into the polymer capsule. Although at pH 5 fluorescence was observed to arise from the Hb residing on the outer surface, at pH 8, it was observed to arise from the polymer capsule interior. Once the Hb is able to diffuse inside the capsule, it gets trapped inside the capsule. Using UV−vis spectroscopy, the extent of protein loading into the polymer capsule was calculated from the absorption at 280 nm (molar extinction coefficient value, ε = 25 565 M^{-1} cm^{-1}). The concentration of confined hemoglobin within polymeric capsule dispersed in 0.1 M PBS was found to be 1 mg mL^{-1}.

SAXS Analysis of the Confined Hb. The synchrotron SAXS was carried out to account for any structural differences between free and confined Hb. The small-angle scattering intensity $I(q)$ of a particle is proportional to the product of the particle form factor $P(q)$ and the structure factor $S(q)$, i.e., $I(q) \propto P(q)*S(q)$. The form factor $P(q)$ is determined by the particle shape (averaged over all orientations), while the structure factor, $S(q)$ term provides information about the interactions and correlations between the particles. However, in dilute solutions such as the present study, the interparticle interactions become negligible and hence $S(q) = 1$. Thus, the form factor can be extracted directly from $I(q)$ versus q data.

For a spherical particle of radius R, the analytical form of $P(q)$ is the following:

$$P(q) = \left[\frac{3\{\sin(qR) - (qR)\cos(qR)\}}{(qR)^3}\right]^2 \quad (1)$$

If the system has a monodisperse size distribution, this equation can be used to extract the radius of the sphere. However, if the system is polydisperse, i.e., possesses spherical particles of varying radii, a size distribution function is introduced into the equation. Experimentally, it has been found that the size distribution in many polydisperse systems can be described using the Schultz distribution function:[13]

$$F(R) = \left[\frac{(Z+1)^{(Z+1)}}{R_{avg}}\right] R_{avg} \exp\left[-\frac{(Z+1)R}{R_{avg}}\right] / \Gamma(Z+1) \quad (2)$$

where R_{avg} is the mean radius, Z is a parameter related to the width of the distribution and this in turn is related to the polydispersity (p) of the distribution as $Z = 1/(p^2 - 1)$, and Γ is the gamma function. The value of p varies between 0 and 1. Thus, the radius of the system is evaluated by fitting the measured scattered intensity to the polydisperse spherical form factor over the whole measured q-range. These R_{avg} and Z values are used to estimate the radius of gyration (R_g) as

$$R_g = \sqrt{\frac{3\langle R^8\rangle}{5\langle R^6\rangle}} = R_{avg}\sqrt{\frac{3(Z+8)(Z+7)}{5(Z+1)^2}} \quad (3)$$

Also,

$$\langle R^N\rangle = \frac{R_{avg}^N}{(Z+1)^N}\frac{(Z+1)!}{Z!} \quad (4)$$

The Porod function used in the analysis of the SAXS pattern is

dx.doi.org/10.1021/jp303596q | J. Phys. Chem. B 2012, 116, 9604−9610

$$I = \frac{B}{q^m} \quad (5)$$

where B is a constant and m is the Porod exponent.

The SAXS profiles recorded for the Hb in solution and the confined Hb dispersed in solution are shown in Figure 3. The

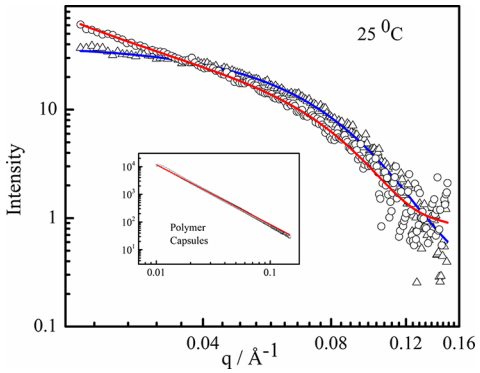

Figure 3. Experimental small-angle X-ray scattering curves obtained at 25 °C in 0.1 M PBS buffer pH 7.0 for 2.5 mg/mL Hb in buffer solution (△) and for Hb confined inside the polymer capsules dispersed in the buffer solution (○). The red (Hb-poly) and the blue (Hb) lines represent the fitted data (see text for details). Inset: SAXS pattern of the polymer capsules fitted using the Porod function (with slope B = 0.63 and m = 1.2).

scattering due to the Hb in solution could be well fitted with polydisperse spheres assuming a Schultz distribution for the number distribution of the sphere sizes. The mean radius of the hemoglobin and the polydispersity factor (p, $0 < p < 1$) obtained from fitting was used to calculate the radius of gyration (R_g) (discussed in detail in the Supporting Information). The radius of gyration (R_g) was estimated to be 43.52 ± 0.87 Å (q range 0.01−0.15 Å^{-1}) using a polydispersity (p) value of 0.71. In the case of the confined Hb (Hb-poly) samples, for $q < 0.03$ Å^{-1}, an additional contribution is observed which is attributed to the polymer capsule matrix. As shown in Figure 3 (inset), the scattering curve due to the polymer capsules could be described with a Porod function valid for the measured q-range (ref 14, Supporting Information, eq 3).The Porod exponent was found to be m = 1.2 (q range 0.01−0.15 Å^{-1}). Using the combined Schultz sphere function and the Porod function in the case of Hb-poly and carrying out the same procedure as that of Hb in solution, the radius of gyration (R_g) of Hb in the confined state comes out to be 26.6 ± 0.65 Å with a low value of p equal to 1.66×10^{-3}. This was attributed to the effect of spherical confinement imposed by the polymer capsule in this case.

To further understand the differences in the state of Hb in solution and in the confined state, the SAXS patterns were compared with their theoretical patterns (Figure 4A and B). The theoretical pattern of Hb was subjected to the same fitting function for polydisperse spheres assuming a Schultz distribution (Supporting Information, Figure S3A). The fitting resulted in a R_g value of 22.32 ± 0.03 Å and polydispersity (p) equal to 0.11. The higher value of R_g compared to the theoretical estimates and literature experimental values (R_g of Hb ~24 Å, obtained using the small-angle neutron scattering technique, ref 15) indicates the presence of Hb aggregation in solution. Further, the high polydispersity (p) value (=0.71)

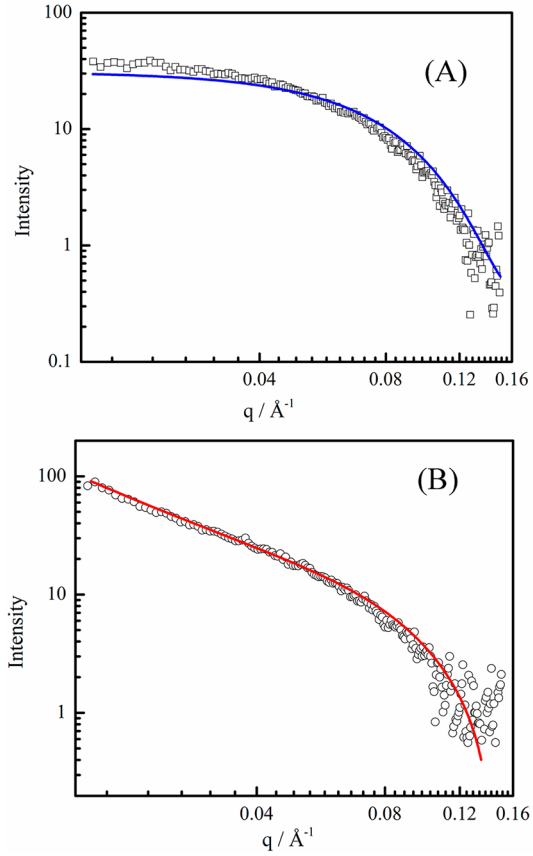

Figure 4. (A) Comparison of the experimental small-angle X-ray scattering pattern (□) for Hb in solution along with the simulated scattering pattern (blue line) generated from atomic coordinates using CRYSOL, (B) Comparison of the experimental small-angle X-ray scattering pattern for Hb confined inside the polymer capsule (○). The line (in red) is the simulated pattern generated from combination of output from CRYSOL and Porod scattering (see text for details).

obtained from the fitting of the experimental data indicates the presence of protein aggregates with varying diameters.

The theoretical SAXS pattern for Hb-poly was generated using the following function:

$$I = I_0 \times \text{Interpolation}(q, q.crysol.I.crysol) + \frac{B}{q^m} + c$$

where Interpolation is a function which determines the intensity at q of the theoretical curve by linear interpolation. I_0, B, m, and c are the fit parameters having values I_0 = 0.614, B = 0.10318, m = 1.609, and c = −2.61. Also, q.crysol, I.crysol were taken from the file generated from CRYSOL using the PDB file 1HHO.

For Hb-poly, the close proximity of the experimental R_g (=26.6 ± 0.65 Å) to the theoretically simulated R_g (=22.37 ± 0.05 Å) suggests that the Hb resides in the nonaggregated state inside the polymer capsules. However, the experimentally obtained value of polydispersity (p) for Hb-poly was much lower compared to Hb in solution and values obtained from theoretical patterns. This probably indicates that, when confined inside polymer capsules, Hb predominantly has a monodispersed size distribution. In the present work, confinement might prevent aggregation of Hb into similar sized clusters but might not guarantee formation of single crystal. This is evident from the larger R_g values compared to the

dx.doi.org/10.1021/jp303596q | J. Phys. Chem. B 2012, 116, 9604−9610

theoretical estimates. The result here thus comprises a convincing example of the beneficial influence of confinement on protein structure. The environment around the Hb, which is largely determined by the functional groups of the polymer capsule, acts as a constraint in terms of space available to the Hb for undergoing aggregation. This effect is further elucidated during the temperature dependent studies.

The temperature dependent SAXS provides information on the change in protein (tertiary) structure with the variation in temperature. In the case of the sample with Hb in solution (Figure 5), with rise in temperature, the R_g value initially

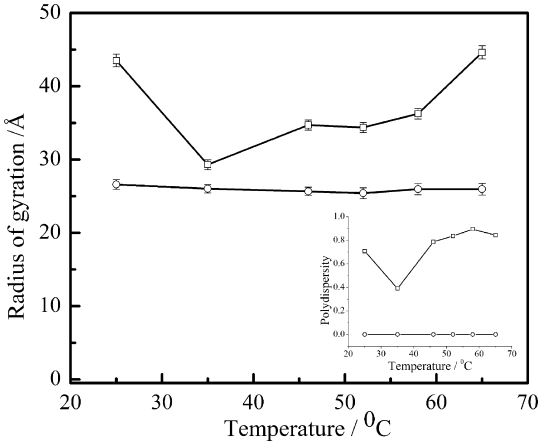

Figure 5. Variation in the radius of gyration, R_g, of Hb in solution (□) and Hb confined within the polymer capsules (○) in the temperature range 25−65 °C. Inset: Variation in the polydispersity factor for Hb in solution (□) and Hb confined within the polymer capsules (○) in the same temperature range.

decreases and thereafter increases with an increase in temperature. This is attributed to the fact that initially at room temperature there is a tendency of the Hb in solution to undergo aggregation in an irregular fashion. As a result of this, although the R_g value is very high, yet due to the unequal sizes of the aggregates in solution, the size distribution is quite broad and the polydispersity value is also quite high. With a rise in temperature, due to the turbulence created by the buffer solution, the aggregates break down, thus leading to formation of smaller aggregates. This causes a drop in both the R_g and p values. With further rise in temperature, Hb gradually unfolds, leading to the formation of aggregates once again and increase in R_g and p values. At very high temperature, when the protein unfolds completely, the extent of aggregation is highest and thus the R_g value is very high. However, since the aggregation proceeds nonuniformly, the aggregate sizes vary over a wide range, leading to a very high value of polydispersity. This is also evident from the change in the SAXS spectra at 58 °C (Supporting Information, Figure S4 and Figure 5, inset). In the case of Hb-poly, the R_g value is observed to be constant and lower over the same temperature range. With a rise in temperature, the Hb trapped within the polymeric layers remains unaffected; i.e., no aggregation takes place. Thus, even if the Hb unfolds, it would be stabilized by the hydrophobic and hydrophilic functional groups on the polymer capsules, preventing it from undergoing aggregation. Thus, the R_g as well as the p value in the case of Hb-poly remains unchanged. On the basis of these results, it can be concluded that the polymer capsule provides a very favorable environment for the Hb molecules which not only prevents it from aggregating but also enables it to withstand higher temperature with very little variation in its structure. Moreover, the configuration of the confined water molecules within the polymer capsules is expected to change with temperature due to the rearrangement of hydrogen bonds.[8] This in turn will influence the orientation of the confined Hb (Hb-poly), resulting in its different behavior compared to that in solution.

Circular Dichroism (CD) Spectroscopy, Thermal Stability, and Electroactivity of Confined Hb. The thermal stability of the Hb in solution and that confined inside the polymer capsule was also probed with circular dichroism (CD) spectroscopy. The melting temperatures of bare and confined Hb were estimated from thermal denaturation curves. The CD signal at 222 nm (n−π^* transition, Figure 6) is monitored in

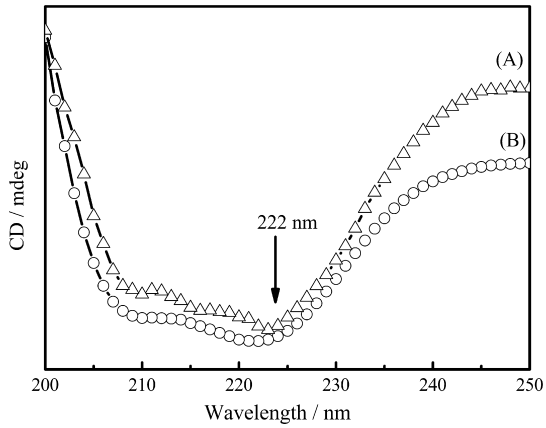

Figure 6. Circular dichroism spectra (CD) at 25 °C for (A) Hb-poly and (B) Hb in 0.1 M PBS buffer (pH 7.0).

the temperature range from 25 to 85 °C, which was then used to obtain a plot of the fraction of unfolded protein (f_u) versus temperature (Figure 7). The denaturation temperature evaluated at f_u = 0.5 was found to be approximately 59 °C in both cases. This shows that Hb is also thermally stable inside the polymer capsule and does not undergo any premature thermal denaturation. The findings from CD are not in one-to-one correspondence with the findings obtained from synchrotron SAXS. This can be attributed to the difference

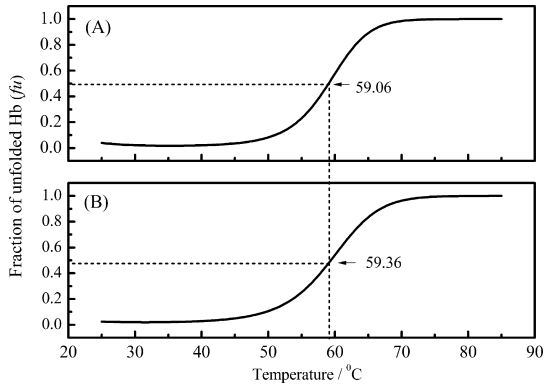

Figure 7. Fraction of unfolded Hb (f_u) in the temperature range from 25 to 85 °C (heating rate = 1 °C min^{-1}) for (A) free Hb in solution (0.1 M PBS, pH 7.0) and (B) Hb confined inside polymer capsules estimated from the variation of the CD signal at 222 nm with temperature.

dx.doi.org/10.1021/jp303596q | J. Phys. Chem. B 2012, 116, 9604−9610

between the techniques. While far-UV CD (<250 nm) probes the secondary structure of the protein, the SAXS essentially probes mostly the tertiary structure. In spite of these differences, the general observations from both studies are the same.

The difference in structural configuration between the bare Hb and Hb-poly samples is also reflected in the protein functions in the form of their electrochemical response. The electrochemical activity of the Hb in solution was compared with the confined Hb (Figure 8) in 0.1 M PBS buffer solution

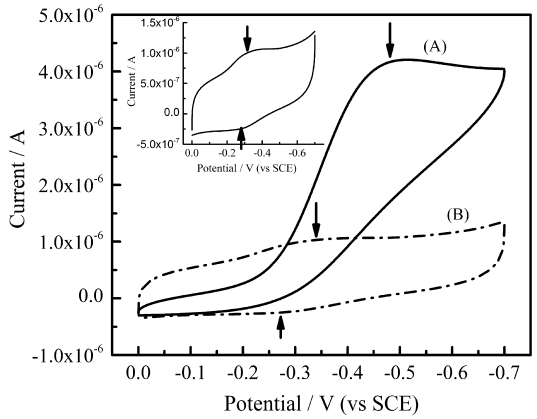

Figure 8. Cyclic voltammogram (at 25 °C) of (A) Hb in solution and (B) Hb-poly in 0.1 M PBS buffer (pH 7.0) at 0.01 V/s. Inset: Magnified voltammogram as in part B.

(pH 7.0) using cyclic voltammetry. It was observed that the Hb/GCE (glassy carbon electrode modified with Hb as working electrode, Pt wire as counter electrode, and SCE as reference electrode) showed only one redox peak at −0.46 V. However, the confined Hb (glassy carbon electrode modified with Hb-poly) showed efficient redox activity with the observation of both the cathodic and anodic peaks at −0.43 and −0.30 V (Figure 8, inset) corresponding to the peaks of Fe^{3+}/ Fe^{2+} in Hb.[16]We suppose that the electroactivity of the Hb in solution and in the confined state can be well correlated to our structural findings obtained from synchrotron SAXS. In the case of Hb in solution, due to protein aggregation, the heme center may take up a position that may be unfavorable for the reversible redox reaction (Fe^{3+} ↔ Fe^{2+}). The aggregation influences the kinetics of charge transfer across the diffuse layer formed close to the electrode, thus favoring one direction of the reversible redox reaction. In the case of the Hb-poly sample, the polymer capsule is composed of chitosan and alginic acid polymer which possess both hydrophobic and hydrophilic groups in their structure. These groups along with the confined water molecules will orient the hydrophobic and hydrophilic fragments of the protein in a way that prevents it from unfolding and hence aggregating. Thus, in the confined state, the heme center takes up orientations favorable for the reversible electrochemical redox reaction. Thus, optimized encapsulation beneficially influences protein structure and hence its function.

CONCLUSION

We have shown here convincingly that confinement of hemoglobin within the polymeric capsules does not have any adverse effects on its structure and function. In fact, confinement resulted in prevention of unwanted aggregation typically observed when the hemoglobin is in solution. This establishes the potential of polymer capsules as protein delivery vehicles in the human body as "bio-encapsulators" for the protein storage. We believe that the conclusions drawn here on confined protein structure can also be extended to account for similar observations for protein confinement inside inorganic matrixes such as silica. Another important implication of this work is the effective usage of synchrotron SAXS to convincingly supplement observation made using other techniques such as electrochemical techniques. Studies such as the present one can be extended to in situ monitoring of protein structural changes taking place during biocatalysis. These would provide a comprehensive understanding of the biophysical processes associated with a particular protein inside a cell.

ASSOCIATED CONTENT

Supporting Information

Schematic diagram showing synthesis of polymer capsules, SEM image of silica sphere, simulated SAXS pattern of Hb fitted using the Schultz sphere function, and SAXS data at 58 °C. This material is available free of charge via the Internet at http://pubs.acs.org.

AUTHOR INFORMATION

Corresponding Author

*E-mail: aninda_jb@sscu.iisc.ernet.in. Fax: +9180 23601310.

Present Address

[§]Department of Biochemistry, University of Calcutta, Kolkata 700019, India.

Notes

The authors declare no competing financial interest.

ACKNOWLEDGMENTS

The authors thank INI (IISc) for TEM, MBU (IISc) for CD studies, and Minakshi Sen (MCBL, IISc) for CLSM imaging. The authors acknowledge the support of the International Centre for Theoretical Physics under ICTP-Elettra Users Program for Synchrotron Radiation.

REFERENCES

(1) Hartmann, M. *Chem. Mater.* **2005**, *17*, 4577.
(2) Hudson, S.; Cooney, J.; Magner, E. *Angew. Chem., Int. Ed.* **2008**, *47*, 8582.
(3) Amar-Yuli, I.; Adamcik, J.; Lara, C.; Bolisetty, S.; Vallooran, J. J.; Mezzenga, R. *Soft Matter* **2011**, *7*, 3348.
(4) O'Brien, E. P.; Stan, G.; Thirumalai, D.; Brooks, B. R. *Nano Lett.* **2008**, *8*, 3702.
(5) (a) Sorin, E. J.; Pande, V. S. *J. Am. Chem. Soc.* **2006**, *128*, 6316. (b) Reátegui, E.; Aksan, A. *J. Phys. Chem. B* **2009**, *113*, 13048. (c) Giovambattista, N.; Rossky, P. J.; Debenedetti, P. G. *J. Phys. Chem. B* **2009**, *113*, 13723.
(6) (a) Ravindra, R.; Zhao, S.; Gies, H.; Winter, R. *J. Am. Chem. Soc.* **2004**, *126*, 12224. (b) Mittal, J.; Best, R. B. *Proc. Natl. Acad. Sci. U.S.A.* **2008**, *105*, 20233. (c) Eggers, D. K.; Valentine, J. S. *Protein Sci.* **2001**, *10*, 250. (d) Cheung, M. S.; Thirumalai, D. *J. Phys. Chem. B* **2007**, *111*, 8250.
(7) Eggers, D. K.; Valentine, J. S. *J. Mol. Biol.* **2001**, *314*, 911.
(8) Reátegui, E.; Aksan, A. *Phys. Chem. Chem. Phys.* **2010**, *12*, 10161.
(9) Fowler, C. E.; Khushalani, D.; Mann, S. *J. Mater. Chem.* **2001**, *11*, 1968.
(10) Hungerford, G.; Benesch, J.; Mano, J. F.; Reis, R. L. *Photochem. Photobiol. Sci.* **2007**, *6*, 152.
(11) Amenitsch, H.; Bernstorff, S.; Kriechbaum, M.; Lombardo, D.; Mio, H.; Rappolt, M.; Laggner, P. *J. Appl. Crystallogr.* **1997**, *30*, 872.

(12) Svergun, D. I.; Barberato, C.; Koch, M. H. J. *J. Appl. Crystallogr.* **1995**, *28*, 768.
(13) (a) Kotlarchyk, M.; Chen, S.-H. *J. Chem. Phys.* **1983**, *79*, 2461. (b) Pontoni, D.; Narayanan, T.; Rennie, A. R. *Langmuir* **2002**, *18*, 56.
(14) Guinier, A.; Fournet, G. *Small-Angle Scattering of X-rays*; John Wiley and Sons: New York, 1955.
(15) Schelten, J.; Schlecht, P.; Schmatz, W.; Mayer, A. *J. Biol. Chem.* **1972**, *247*, 5436.
(16) Kapoor, S.; Mandal, S. S.; Bhattacharyya, A. J. *J. Phys. Chem. B* **2009**, *113*, 14189.